THERMAL PROPERTIES OF 2D MOLYBDENUM DISULFIDE

Jifen Wang[1], Huaqing Xie[1] and Zhixiong Guo[2]

[1] School of Science, College of Art and Science, Shanghai Polytechnic University
No.2360 Jinhai Rd., Shanghai 201209, China
wangjifen@sspu.edu.cn; hqxie@sspu.edu.cn

[2] Department of Mechanical and Aerospace Engineering, Rutgers, The State University of New Jersey
Piscataway, NJ 08854, USA
guo@jove.rutgers.edu

Abstract. The first principle is used to optimize the structure of molybdenum disulfide layers and to calculate the thermal and optical properties. The results include the heat capacity, vibrational entropy, totally electronic energy, Helmholtz free energy and the IR and Raman spectra of molybdenum disulfide layers. The results show that the number of layers of is more important to the thermal properties of molybdenum disulfide than the size of layers.

1. Introduction

In recent years, two-dimensional nanomaterials represented by graphene have aroused extensive interest in the field of micro-nano-electronics. People are very concerned about what materials can replace silicon as the basic materials for the next generation of large-scale integrated circuits[1]. Graphene was once the focus of attention, but its bandgap free band structure was not suitable for making circuits. Therefore, molybdenum disulfide (MoS_2), which has similar structural properties but is more excellent in band structure, has gradually become a hot topic in the research of new semiconductor materials[2]. The bulk material MoS_2 is an indirect bandgap semiconductor with the forbidden band width of 1.29 eV. While monolayer MoS_2 has a direct bandgap semiconductor with the forbidden band width of 1.8 eV[3]. In the MoS_2 layer, S^{2-} and Mo^{4+} are connected with each other by strong covalent bond, while the normal force between MoS_2 layer and MoS_2 layer is weak[4]. Therefore, lithium and magnesium plasma can be effectively inserted into the MoS_2 sheet layer. Therefore, MoS_2 is widely concerned in the cathode materials of lithium and magnesium ion batteries[5]. Radisavljevic et al. successfully separated the layered MoS_2 by microcomputer separation method. Moreover, they successfully transplanted the separated MoS_2 onto the SiO_2/Si substrate[6]. Up to now, there have been a lot of theoretical and experimental studies on the electronic structure and surface properties of MoS_2 materials, but few studies have been conducted on its optical properties, especially the optical properties of single-layer MoS_2. In recent years, first-principles methods based on density functional (DFT) theory have been increasingly used to calculate the optical properties of materials.

In this article, we use the DFT theory compose and cast a shadow under the framework of the plane wave method, using the local density approximation, the single MoS_2 band structure, density of states and optical properties, such as energy loss spectrum, absorption coefficient and reflectivity, refractive index and extinction coefficient to compare the comprehensive plan, and the results are compared with the existing theoretical results.

2. Theoretical details

The present calculations were carried out by VASP code [7, 8], which is a complex package for performing ab-initio quantum-mechanical molecular dynamics (MD) simulations based on first-principles density functional theory (DFT). For calculation of a system, the approach implemented in VASP is based on the (finite-temperature) local-density approximation with the free energy as variable quantity and an exact evaluation of the instantaneous electronic ground state at each MD time step. VASP uses efficient matrix diagonalization schemes and an efficient Pulay/Broyden charge density mixing. These techniques avoid all problems possibly occurring in the original Car-Parrinello method [9], which is based on the simultaneous integration of charged particles, both electronic and ionic, equations of motion. The interaction between them is described by ultra-soft Vanderbilt pseudopotentials (US-PP) [10] or by the projector-augmented wave (PAW) method. US-PP (and the PAW method) allows for a considerable reduction of the number of plane-waves per atom for transition metals and first row elements.

The heat capacity of MoS_2, C_v, is represented in terms of contributions of all atoms and possible directions by

$$\mathrm{C_v} = \sum_{\mathrm{i,\mu}} \mathrm{C_{i,\mu}} \tag{1}$$

$$C_{i,\mu} = dk_B \int g_{i,\mu,}(\omega) \left(\frac{\hbar\omega}{2k_BT}\right)^2 \frac{\exp(\frac{\hbar\omega}{k_BT})}{\left(\exp\left(\frac{\hbar\omega}{k_BT}\right)-1\right)^2} d\omega \tag{2}$$

In which, $C_{i,\mu}$ is the contribution of any atom in any possible direction to the heat capacity. T is temperature in Kelvin, k_B is Boltzmann constant, and h is Planck constant. At the low and high temperature limits, we have

$$\lim_{T\to 0} C_{i,\mu} = 0, \ \lim_{T\to\infty} C_{i,\mu} = k_B \tag{3}$$

The Helmholtz free energy of a unit cell, A_T, is in harmonic approximation

$$\mathrm{A_T} = \sum \mathrm{A_{i,\mu}} \tag{4}$$

$$A_{i,\mu} = dk_BT \int_0^\infty g_{i,\mu,}(\omega) \ln\left(2\sin\frac{\hbar\omega}{k_BT}\right) d\omega \tag{5}$$

The entropy of a unit cell, S_T, is described by

$$S_T = \sum_{i,\mu} S_{i,\mu} \tag{6}$$

$$S_{i,\mu} = dk_B \int_0^\infty g_{i,\mu,}(\omega) \left(\frac{\hbar\omega}{2k_BT}\left(\cos\left(\frac{\hbar\omega}{2k_BT}\right)-1\right) - \ln\left(1-\exp(\frac{-\hbar\omega}{k_BT})\right)\right) d\omega \tag{7}$$

Internal energy is the total kinetic energy of a thermodynamic system, which is the energy due to motion of particles, including rotational, translational, and vibrational motion. The potential energy is associated with the vibrational energy of atoms within given molecules or crystals. It includes energy in all of chemical bonds in a system, and the energy of the free electrons or conduction electrons in metals. In this work, the total energy (E_T) at temperature T is the electronic energy of formation plus the vibrational internal energy, i.e., $E_T = E_{elec} + ZPE + E_{vib(T)}$, where ZPE is the zero point energy. $E_{vib(T)} = E_T - E_0$ is the change in vibrational internal energy from 0 K. The following relationship holds between the Helmholtz free energy, total energy, and entropy:

$$A_T = E_T - TS_T \quad (8)$$

In the present simulations, the phonon spectra were calculated on an optimized structure by DFT. All the DFT calculations have been performed in the framework of generalized gradient approximation (GGA) technique considering the exchange and correlation functional as proposed by Perdewe-Burkee-Ernzerhof (PBE) [11]. There is no magnetic moment in the present model, and the default plane wave cutoff energy is 500 eV. The electronic iterations convergence is 1.00×10^{-5} eV using the blocked Davidson algorithm and reciprocal space projection operators. Fig. 1. is the top view and side view of calculated double layers MoS_2. In the calculation, we used the first order Methfessel-Paxton smearing with a width of 0.2 eV and the k-spacings of 0.383 ◊0.383 ◊ *c* per Angstrom for the monomer(1), double layers(2) and four layers MoS_2(4). The big size of double layers MoS_2 (2-1) is four times of side length in top view, that is 4a×4b when the top views of 1,2,4 are a×b.

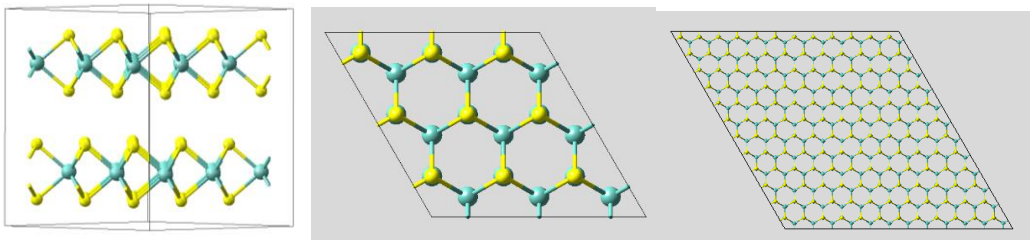

Fig. 1. Views of MoS_2: side view of 2 (left); top view of 1, 2, 4(middle); top view of 2-1(right)

3. Results and discussion

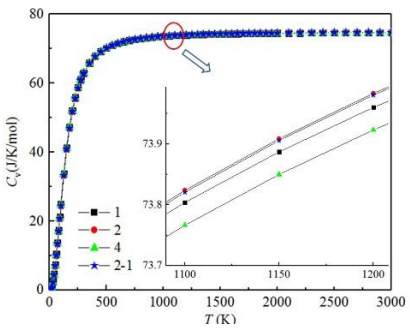

Fig. 2. The C_v curves of the MoS_2 layers

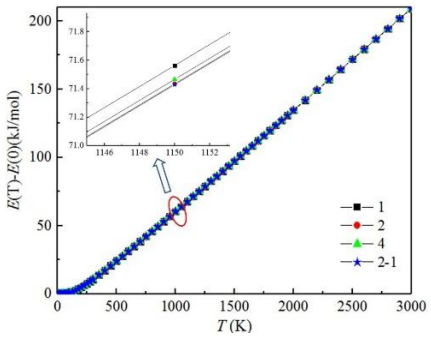

Fig. 3. The *E*(T)-*E*(0) curves of the MoS_2 layers

Fig.2 shows the results of the C_v curves of the MoS_2 layers. In the figure, 1, 2, 4 and 2-1 are the monolayer, double layers, four layers and double layers with four cells of MoS_2, respectively. The C_v curves in the figure have the same trend. can be described in three stages as temperature changes. C_v MoS_2 can be described in three stages as temperature changes. Firstly, C_v of MoS_2 increases rapidly with the increase of temperature when temperature is lower than 500 K. Secondly, at 500 to 1000 K, C_v of MoS_2 increases slow with temperature. The curves of C_v are almost parallel to the temperature at the temperature higher than 1000K. In other words, C_v does not increase with temperature any longer at high temperature. As can be seen in the locally enlarged image, C_v of monolayer MoS_2 is higher than that of four layers

MoS_2 and lower than that of double layers MoS_2 at the same temperature, such as 1100 K. At the same temperature, the difference C_v of double layers MoS_2 between one cell and four cells is very small, which is about 0.01J/mol/K.

Fig. 3 shows the E(T)-E(0) curves of the MoS_2 layers. In this figure, there is a trend chart contrary to C_v curves. E(T)-E(0) of MoS_2 layers increase slowly at low temperature while rapidly at high temperature. At the same temperature, such as 1150K, the highest E(T)-E(0) is for monomer MoS_2 while the lowest is for the double layers. It might be mean that the monomer MoS_2 is less stable than the others in the work and the double layer ones are the most stable MoS_2. The two kinds of double layers have very close data of E(T)-E(0). The lowest E(T)-E(0) in the figure is for the big cell of double layers MoS_2. Therefore the number of layers has great influence on E(T)-E(0) of MoS_2 layers, while the size has little influence on E(T)-E(0) of MoS_2 layers.

The curves of S(T) for the MoS_2 layers are shown in Fig.4. As shown in the figure, there is a increase trend for S(T) of the MoS_2 layers with temperature. curves of S(T) for the MoS_2 layers are going up slowly at lower temperature than 100 K. It increases quickly when temperature is from 100 ~1000 K. The slope of the curves get smaller and smaller when temperature is higher than 1000 K. In a locally enlarged view, the monomer has highest S(T). The double layers MoS_2 has lowest S(T). The difference of S(T) between the two kinds double layers MoS_2 is smaller than that between MoS_2 with different layers. So the number of layers is is critical to S(T) of MoS_2 layers.

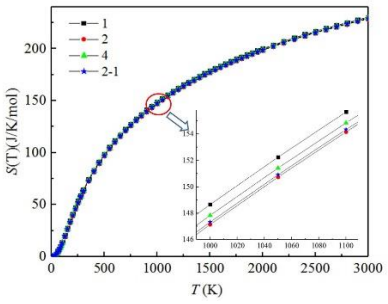

Fig. 4. The S(T) curves of the MoS_2 layers

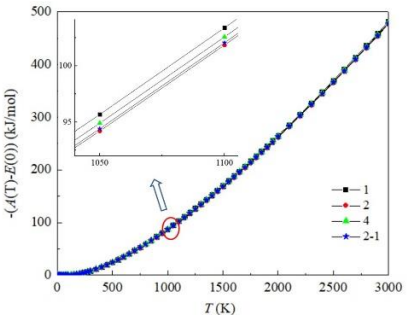

Fig. 5. The –(A(T) -E(0))curves of the MoS_2 layers

The –(A(T) -E(0)) curves of the MoS_2 layers were shown in Fig. 5. In the figure, the –(A(T) -E(0)) of MoS_2 layers increase with temperature. The curves of the MoS_2 layers are flat at low temperature while the slope of curves gets steeper and steeper at the temperature above 250 K. In the local enlarged view, –(A(T) -E(0)) of monomer MoS_2 is highest and that of double layers. The big cell of the double layers has a higher –(A(T) -E(0)) than the small cell double layers MoS_2. The difference of –(A(T) -E(0)) between the double layers MoS_2 is very small. Therefore size has little effect on –(A(T) -E(0)), compared with number of layers.

Fig. 6 shows the A(T) curves of the MoS_2 layers. The figure shows that there is a trend of decrease A(T) with temperature. The curves of A(T) are almost flat before 250 K. They began to decrease and speed up to reduce with temperature at higher temperature than 250 K. In the partly enlarged view, the lowest A(T) is for the monomer MoS_2 in the figure. The double layers MoS_2 have high A(T) than the fours layers at the same temperature.

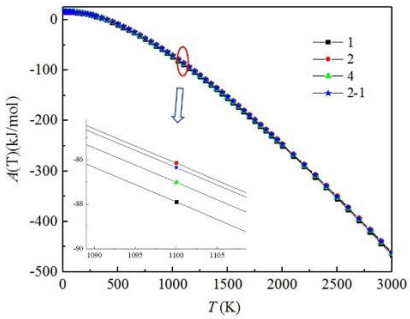

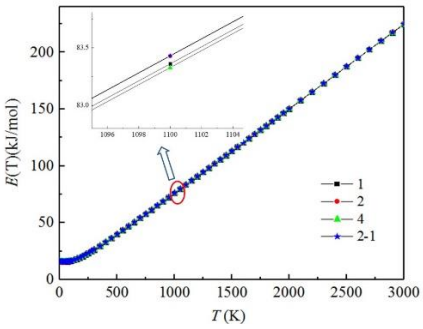

Fig. 6. The *A*(T) curves of the MoS_2 layers **Fig. 7.** The *E*(T) curves of the MoS_2 layers

E(T) curves of the MoS_2 layers were shown in Fig. 7. In the figure, the slope of curves is getting more and more negative. In low temperature, the *E*(T) of the MoS_2 layers decrease slightly while accelerate the decline at the temperature above 250 K. *E*(T) decrease to lower than -450 kJ/mol. In the partly enlarged view, the monomer MoS_2 has the lowest *A*(T). The highest *A*(T) in the figure is for the double layers MoS_2. Two kinds double layers MoS_2 have similar value in *A*(T) and the big cell has the lower *A*(T) at the same temperature. The number of layers play a leading role on *A*(T) of the MoS_2 layers.

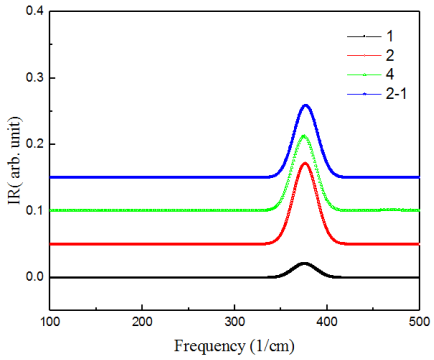

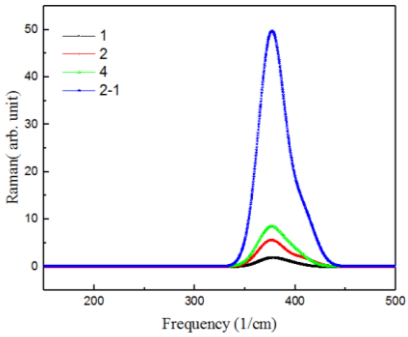

Fig. 8. The IR of the MoS_2 layers **Fig. 9.** The Raman of the MoS_2 layers

Fig.8 describes the IR spectra of the MoS_2 layers and Fig.9 describes the Raman spectra of the MoS_2 layers. In the figures, the positions of the peaks are almost identical. In the IR spectra, there is not much difference in peak height except for the low peak of monomer MoS_2. In Raman spectra, the difference of peak height was obvious, which low to high order is 1, 2, 4, 2-1. There are shoulder seam marks on the right side of the main peak in the Raman spectra.

4. Conclusions

The less layers of MoS_2 was simulated by first principle and calculated thermal properties of the layers. The results showed that C_v of MoS_2 layers increases with temperature and the slope of the curves is steep at temperature lower than 500 K and tend to be flat at temperature

higher than 1000 K. The monomer MoS_2 had a higher C_v than four layers MoS_2 and a lower C_v than double layers MoS_2. $E(T)$-$E(0)$ and $E(T)$ increase with temperature. The slop of $E(T)$-$E(0)$ and $E(T)$ curves has a gradually steep trend. $-(A(T)-E(0))$ curves of MoS_2 layers show a trend of acceleration with temperature. The monomer has the highest $-(A(T)-E(0))$ at the same temperature. $A(T)$ curves of MoS_2 layers have countertrend with those of $-(A(T)-E(0))$. The $S(T)$ of MoS_2 layers has an increasing slop at low temperature and a decreasing slop at high temperature. The monomer has the highest $S(T)$ at the same temperature. In IR and Raman spectra, the MoS_2 layers have almost peak position but different in peak height. The number of layers play more important role in thermal properties of MoS_2 layers than the size does. The double layers MoS_2 is the most stable.

Acknowledgements

This work was supported by the National Natural Science Foundation of China (No. 51776116); The Major Program of the National Natural Science Foundation of China (No. 51590902); Gaoyuan Discipline of Shanghai – Environmental Science and Engineering (Resource Recycling Science and Engineering.

References

[1] B. Tian, X. Zheng, T.J. Kempa, Y. Fang, N. Yu, G. Yu, J. Huang, C.M. Lieber, Coaxial silicon nanowires as solar cells and nanoelectronic power sources, Nature, 449 (2007) 885.

[2] M. Chhowalla, D. Jena, H. Zhang, Two-dimensional semiconductors for transistors, Nat Rev Mater, 1 (2016) 16052.

[3] S.Z. Butler, S.M. Hollen, L. Cao, Y. Cui, J.A. Gupta, H.R. Gutiérrez, T.F. Heinz, S.S. Hong, J. Huang, A.F. Ismach, E. Johnston-Halperin, M. Kuno, V.V. Plashnitsa, R.D. Robinson, R.S. Ruoff, S. Salahuddin, J. Shan, L. Shi, M.G. Spencer, M. Terrones, W. Windl, J.E. Goldberger, Progress, Challenges, and Opportunities in Two-Dimensional Materials Beyond Graphene, Acs Nano, 7 (2013) 2898-2926.

[4] N. Mounet, M. Gibertini, P. Schwaller, D. Campi, A. Merkys, A. Marrazzo, T. Sohier, I.E. Castelli, A. Cepellotti, G. Pizzi, N. Marzari, Two-dimensional materials from high-throughput computational exfoliation of experimentally known compounds, Nature Nanotechnology, 13 (2018) 246-252.

[5] M. Heiranian, A.B. Farimani, N.R. Aluru, Water desalination with a single-layer MoS2 nanopore, Nature Communications, 6 (2015) 8616.

[6] B. Radisavljevic, A. Radenovic, J. Brivio, V. Giacometti, A. Kis, Single-layer MoS2 transistors, Nature Nanotechnology, 6 (2011) 147.

[7] G. Kresse, J. Hafner, Abmolecular dynamics for liquid metals, Phys Rev B, 47 (1993) 558-561.

[8] G. Kresse, J. Furthmuller, Efficient Iterative Schemes for Ab Initio Total-Energy Calculations Using a Plane-Wave Basis Set, Phys Rev B, 54 (1996) 11169-11186.

[9] R. Car, M. Parrinello, Unified Approach for Molecular Dynamics and Density-Functional Theory, Phys Rev Lett, 55 (1985) 2471.

[10] D. Vanderbilt, Soft self-consistent pseudopotentials in a generalized eigenvalue formalism, Phys Rev B, 41 (1990) 7892.
[11] J.P. Perdew, K. Burke, M. Enzerhof, Generalized Gradient Approximation Made Simple, Phys Rev Lett, 77 (1996) 3865-3868.